Polarized Electronic Spectra of Single Crystals of Glutarimide

Shimin Xu and Leigh B. Clark*

Contribution from the Department of Chemistry and Biochemistry, University of California, San Diego, 9500 Gilman Drive, La Jolla, California 92093-0359

Received April 12, 1994®

Abstract: Reflection spectra for radiation polarized along the *a*, *b*, and *c* crystal axes of the (100) and (001) faces of single crystals of glutarimide have been measured between 500 and 140 nm. Corresponding absorption spectra are obtained through Kramers–Kronig analysis of the reflection data. Three transitions are assigned as follows: I, 40 200 cm^{-1} (249 nm), $f = 0.001$, $n\pi^*$, polarized perpendicular to the plane of the imide linkage; II, 44 800 cm^{-1} (223 nm), $f = 0.007$, $n\pi^*$, polarized perpendicular to the mirror plane; and III, 49 800 cm^{-1} (201 nm), $f = 0.30$, $\pi\pi^*$, polarized perpendicular to the mirror plane. Additional absorption is observed around 70 000 cm^{-1} in the crystal spectra but the spectra cannot be uniquely decomposed into individual bands owing to its diffuse nature. The two weak, lower energy transitions (I and II) are derived mainly from carbonyl $n\pi^*$ transitions. Semiempirical MO calculations (INDO/S-CI) predict two weak $n\pi^*$ bands followed by a moderately intense $\pi\pi^*$ transition with the observed excited state symmetries. The calculations lead to a satisfactory fit for the energy of the $\pi\pi^*$ band but underestimate the energies of the $n\pi^*$ bands by about 10 000 cm^{-1}.

Introduction

Glutarimide (2,6-piperidinedione) is a component in a number of molecules with interesting biochemical activity. For example, many substituted glutarimides exhibit properties of partial agonists in the central nervous system.[1] Antineoplaston A10 (3-[(phenylacetyl)amino]-2,6-piperidinedione) has been reported to have anticancer activity.[2-4] Glutarimide is also a structural part of the glutarimide antibiotics, such as actiketal,[5] lactimidomycin,[6] and epiderstatin.[7] In spite of the apparent chemical importance of glutarimide and the imide group in general, little has been done to characterize the electronic propeties of this chromophore.[8] The purpose of the present work is to explore the electronic structure and spectrum of glutarimide and to provide experimental values for several spectroscopic parameters (transition energies, oscillator strengths, transition moment directions) of the imide linkage. These results for the imide group contribute to a growing data base of electronic spectral properties for fundamental chromophores and can be used in testing and in directing the development of theoretical molecular orbital methods for such molecules.

Glutarimide is a small molecule with C_S symmetry. The molecular framework is planar except for the central carbon opposite the nitrogen. If we ignore the nonplanarity, then the local point group of the imide region is C_{2v} (Figure 1). Generally in what follows we will assume local C_{2v} symmetry in order to simplify the spectroscopic assignments. By convention[9,10] the 2-fold axis is chosen as *z*, while the direction normal to the plane is taken as *y*.

Available information regarding the electronic spectrum of the imide group is scant. Turner observed a band at 50 000 cm^{-1} (200 nm) with a maximum extinction coefficient of 13 000 L mol^{-1} cm^{-1} for glutarimide in acetonitrile solution. He also reported a similar band at 51 300 cm^{-1} for succinimide and some of its alkyl derivatives.[8] The simplest valence shell orbital scheme for the imide linkage gives five π type orbitals along with two nonbonding orbitals. The six π electrons and the four nonbonding electrons of this system are expected to appear as in Figure 1, and the imide absorption band observed by Turner is presumably the $\pi_3 \rightarrow \pi_4^*$ transition. Turner made no mention of any $n\pi^*$ transitions.

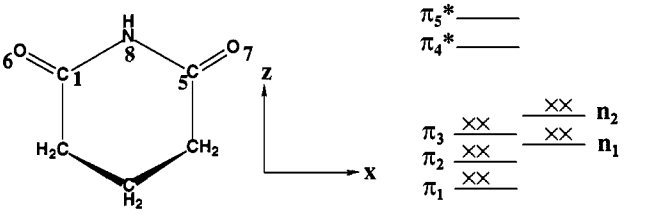

Figure 1. (Left) Structure of glutarimide and molecular coordinate system and (right) expected orbital energy level scheme for the π and nonbonding molecular orbitals.

In order to determine the ordering of the orbitals and to assign transitions, information concerning the excited state symmetries of the observed bands is essential. These symmetries are derivable from the directions of the transition moment vectors, and the latter can be obtained from polarized absorption spectra of oriented samples, *viz.* single crystals. Crystals of glutarimide are easily grown from water solution and are stable in the laboratory environment. The other candidate for this study, succinimide, exhibited fairly rapid crystal deterioration and was therefore rejected.

The imide linkage is one example of a group of fundamental chromophores that are made from C, N, and O atoms and that do not exhibit formal structural resonance. The spectra of these chromophores generally appear in the vacuum ultraviolet, and little experimental information about such systems is available. This paper is the second contribution (following a paper on urea)[11] in a program aimed at characterizing the excited states of these fundamental chromophores. On the basis of the orbital energy diagram our expectation for the low-energy region is that glutarimide should exhibit strong $\pi \rightarrow \pi^*$ bands (at least one)

* To whom correspondence should be addressed.

® Abstract published in *Advance ACS Abstracts*, September 1, 1994.

(1) Laycock, G. M.; Shulman, A. *Nature* **1967**, *213*, 995.
(2) Burzynski, S. R. *Adv. Exp. Clin. Chemother.* **1988**, *6*, 45.
(3) Hendry, L. B.; Muldoon, T. G. *J. Steroid Biochem.* **1988**, *30*, 325.
(4) Michalska, D. *Theochem.* **1991**, *231*, 357.
(5) Sonoda, T.; Osada, H.; Uzawa, J.; Isono, K. *J. Antibiot.* **1991**, *44*, 160.
(6) Sugawara, K.; Nishiyama, Y.; Toda, S.; Komiyama, N.; Hatori, M.; Moriyama, T.; Sawada, Y.; Kamei, H.; Konishi, M.; Oki, T. *J. Antibiot.* **1992**, *45*, 1433.
(7) Sonoda, T.; Kobayashi, K.; Ubukata, M.; Osada, H.; Isono, K. *J. Antibiot.* **1992**, *45*, 1963.
(8) Turner, D. W. *J. Chem. Soc.* **1957**, 4555.
(9) Wilson, E. B., Jr.; Decius, J. C.; Cross, P. C. *Molecular Vibrations*; McGraw-Hill: New York, 1955.
(10) Robin, M. B. *Higher Excited States of Polyatomic Molecules*; Academic: New York, 1974; Vol. I.
(11) Campbell, B. F.; Clark, L. B. *J. Am. Chem. Soc.* **1989**, *111*, 8131.

0002-7863/94/1516-9227$04.50/0

and, if sufficiently removed from the midst of stronger absorption, two approximately degenerate, weak bands arising from the $n \rightarrow \pi^*$ transitions of the two carbonyl groups.

Apart from the brief work reported by Turner in 1957,[8] we have not seen any report of experimental or theoretical work on the electronic spectrum of glutarimide or imides in general. In this paper, we present the polarized electronic spectra of crystalline glutarimide from 500 to 140 nm. The direct measurement of absorption spectra of strongly absorbing crystals is nearly impossible, owing to the extreme sample thinness required, and consequently we derive absorption curves from experimental reflection spectra through Kramers–Kronig analysis. We also give the results of MO calculations using the intermediate neglect of differential overlap/configuration interaction (INDO/S-CI).

Experimental Section

Glutarimide (98%) was purchased from Aldrich Chemical Co. and was used without further purification. Crystals were grown by slow evaporation from aqueous solutions. Typical crystals were about 3 × 1 × 0.5 mm. The crystal structure of glutarimide has been reported by Petersen as monoclinic (space group $P2_1/c$) with four molecules per cell.[12] The crystals obtained here were elongated along the b axis. Miller indices were determined from morphologic examination of interfacial angles and were confirmed by X-ray diffraction methods. Some crystals showed the (001) face as predominant (described by Petersen[12]), while most crystals exhibited (100) as the principal face. The latter face shows excellent cleavage. The molecular framework (excepting the central methylene) lies close to the (001) crystal plane.

The surface quality of the natural faces was not sufficient for making accurate reflectivity measurements. Excellent surfaces of the (100) face were prepared simply by cleaving individual crystals. Suitable surfaces of the (001) face were prepared by polishing with an ultramicrotome. For this procedure a crystal of suitable size was epoxied to one end of a brass rod that was mounted in the specimen holder of an ultramicrotome (LKB Model 4802A). The arcs of the specimen holder were adjusted so that the (100) face was oriented close to perpendicular to the diamond knife blade of the ultramicrotome, and initial coarse cuts were made using the mechanical feed. After some initial cutting strokes, final adjustment of the orientation of the face was made by examining the angles the new "cut face" made with the natural (100) boundaries. On occasion the specimen holder was dismounted, and the crystal was examined with a microscope to confirm the orientation of the polished face. When it was determined that the desired face was, in fact, perpendicular to the knife blade, final polishing was accomplished by advancing the crystal using the thermal feed of the ultramicrotome. A typical feed rate of 200 Å per stroke was applied, and the face was polished for about 30 min. The polished face thus prepared was highly reflective and free of visible imperfections.

Reflection spectra between 500 and 140 nm were measured from both freshly cleaved (100) faces and polished (001) faces. The two instruments used for the reflection measurements and the procedures employed in the Kramers–Kronig transformation have been described previously.[11,13] Aqueous and trimethyl phosphate (TMP, 99+%, Aldrich) solution spectra were measured using a nitrogen-flushed, Olis-modified Cary 15 spectrophotometer.

Computations

The MO calculations reported here used a spectroscopic version of the intermediate neglect of differential overlap configuration interaction (INDO/S-CI) package[14-17] kindly provided by Professors Patrik Callis of Montana State University and Michael Zerner of the University of Florida. The program provides standard electron repulsion parameters such as Mataga–Nishimoto (MN),[18] Ohno–Klopman (OK),[19] and Pariser.[20] The interaction scaling factors f_σ and f_π, which affect the splitting between bonding and antibonding MO's, may be adjusted conveniently. Up to 210 singly and/or doubly excited configuration may be included in the configuration interaction calculation.[17] These programs were edited to run on a 486DX2 microprocessor-based PC.

In the calculations reported here, we have used two representative parameter sets which have been applied usefully to many heteroaromatic systems.[17] The two sets are referred to as singly excited (SCI) and singly and doubly excited (SDCI) configuration interactions here. Both SCI and SDCI use INDO/1 parameters. SCI uses MN electron repulsion parameters with the traditional interaction scaling factors $f_\sigma = 1.267$ and $f_\pi = 0.585$ and no energy selection.[17] SDCI uses OK electron repulsion with $f_\sigma = 1.1$ and $f_\pi = 0.55$. For the SDCI calculations, only $\pi\pi^*$ singly and doubly excited configurations are included. Moreover, a criterion was used to reduce the number of configurations entering into the configuration interactions. Only the configurations consisting of sets i and j selected from CI Hamiltonian matrix elements such that $H_{ii} < 80\,000$ cm^{-1} and $|H_{ij}/(H_{ii} - H_{jj})| > 0.02$ were admitted. In this way higher energy configurations are excluded from the configuration interaction calculations.

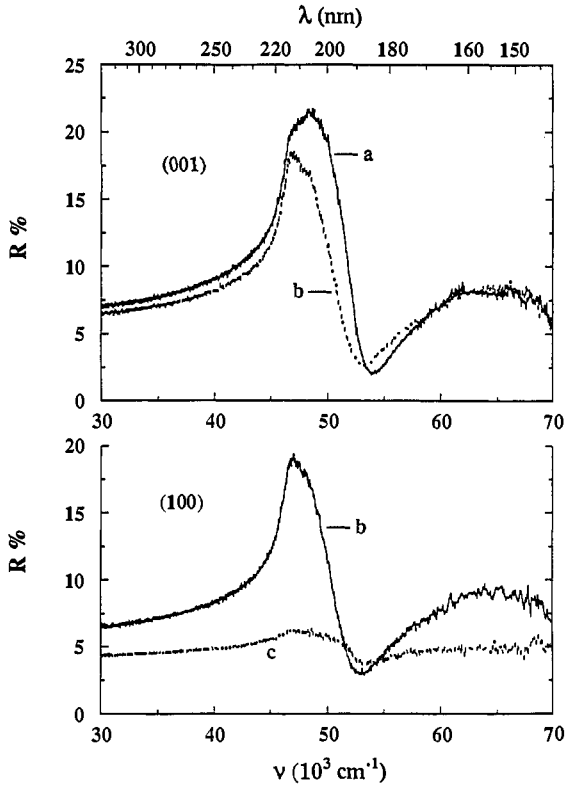

Figure 2. (Top) Reflection spectra for light polarized along the a (solid line) and b (dashed line) axes of (001) and (bottom) the b (solid line) and c (dashed line) axes of (100) face.

Results and Interpretation

Spectra. Reflection spectra polarized along the a, b axes of the (001) face and b, c axes of the (100) face are shown in Figure 2. The spectra polarized along the b axis from two faces are almost identical. This result is of course required by crystal symmetry and verifies that no observable disordering of the lattice has occurred owing to the polishing procedure employed for (001). The absorption spectra obtained from the Kramers–Kronig transformations of the three reflection spectra are shown in Figure 3. The transformation procedure requires extrapolation of each

(12) Petersen, C. S. *Acta Chem. Scand.* **1971**, *25*, 379.
(13) Zaloudek, F.; Novros, J. S.; Clark, L. B. *J. Am. Chem. Soc.* **1985**, *107*, 7344.
(14) Ridley, J.; Zerner, M. C. *Theor. Chim. Acta* **1973**, *32*, 111.
(15) Edwards, W. D.; Ohrn, N. Y.; Weiner, B. L.; Zerner, M. C. *Int. J. Quantum Chem. Symp.* **1984**, *18*, 507.
(16) Parkinson, W. A.; Zerner, M. C. *J. Chem. Phys.* **1991**, *94*, 478.
(17) Callis, P. R. *J. Chem. Phys.* **1991**, *95*, 4230.
(18) Mataga, N.; Nishimoto, K. *Z. Phys. Chem. (Frankfurt)* **1957**, *13*, 140.
(19) Klopman, G. *J. Am. Chem. Soc.* **1964**, *86*, 4550.
(20) Pariser, R.; Parr, R. G. *J. Chem. Phys.* **1953**, *21*, 767.

Table 1. Solution and Crystal Spectral Data for Glutarimide from Experiments[a]

	water solution		TMP solution		*a* axis		*b* axis		*c* axis	
	f	ν (cm^{-1})	*f*	ν (cm^{-1})	*f*	ν (cm^{-1})	*f*	ν (cm^{-1})	*f*	ν (cm^{-1})
I	0.0010	40 200	0.0010	39 700	~0.005	38 900	~0.005	39 000	~0.005	41 000
II	0.0072	44 800	0.0027	44 700	0.032	45 100	0.026	44 800	0.012	44 400
III	0.30	49 800	0.27	50 000	0.58	49 500	0.44	48 800	0.13	52 200

[a] Oscillator strengths from solution spectra are randomized three-dimensional values. Crystal values are one-dimensional.

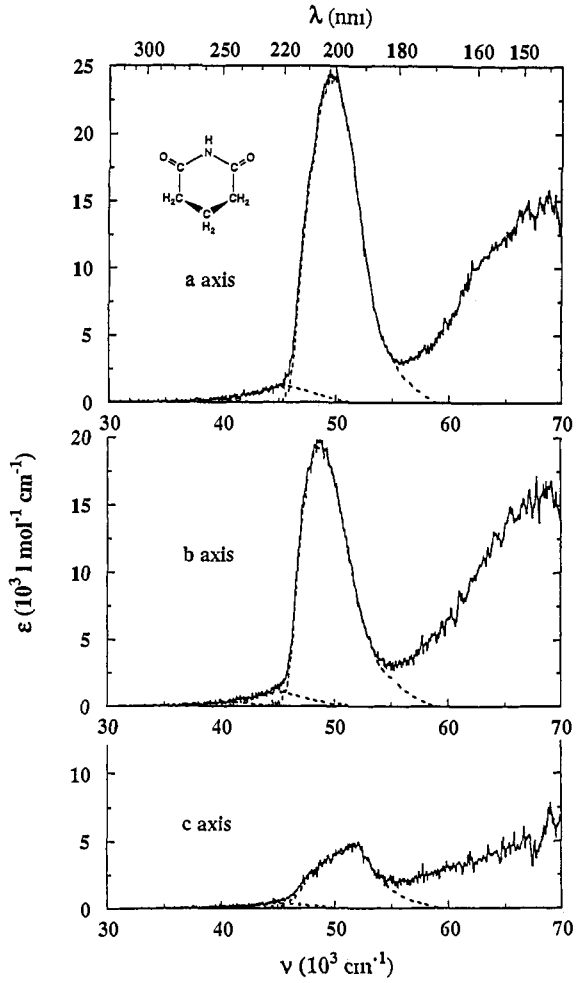

Figure 3. Absorption spectra for light polarized along the *a*, *b*, and *c* axes obtained from Kramers–Kronig transformations of the corresponding reflection spectra. The dashed bands represent plausible resolutions into components.

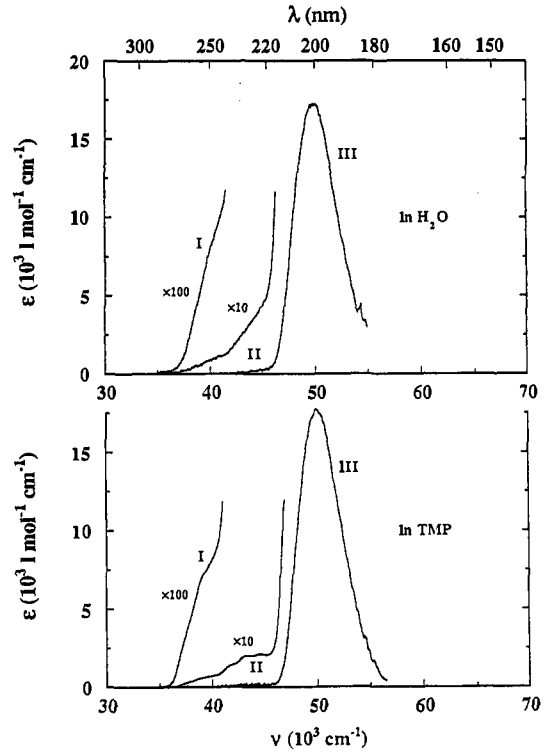

Figure 4. (Top) Aqueous solution spectrum of glutarimide and (bottom) spectrum of glutarimide dissolved in trimethyl phosphate. Roman numerals designate the three transitions.

measured reflection spectrum both to higher and lower frequency. These assumed "trial" regions are adjusted in a systematic way until the transformed spectrum shows essentially zero computed absorption throughout the known transparent spectral region. In addition, the output is required to be consistent with directly measured absorption edge values as well. By using these criteria it is found that different trial region extensions can lead to equally acceptable transformations. Once the criteria are met, then the variation of the calculated absorption curves throughout the experimentally measured region is negligible irrespective of the particular shape of the trial region extensions. We conclude that the resulting absorption spectra are insensitive to the details used in the trial regions.

For the absorption edge determination, a thin slice of freshly cleaved crystal (mounted over a pinhole) was inserted into a rotatable holder mounted in the Cary spectrophotometer. Absorption edges were measured parallel to both the *b* and *c* axes using a calcite polarizer. The onset of absroption occurs at about 36 000 cm^{-1} for light polarized along both axes, and this information was used in the Kramers–Kronig transformation procedures. The absorption spectra in both TMP and aqueous solutions are displayed in Figure 4.

Resolving individual band components for the one strong band in each spectrum was straightforward. On the other hand, it was not possible to unambiguously decompose the lower energy region (36 000–47 000 cm^{-1}) into two individual components, owing to the general weakness of the absorption. Because the solution spectra clearly exhibit two very weak transitions in this region, we have correspondingly resolved two bands with similar relative positions from each absorption spectrum in this lower energy region (see Figure 3). The absorption region above 60 000 cm^{-1} is noisy and diffuse. It is likely that there are multiple, overlapped transitions composing this region, and no attempt has been made at an analysis in terms of individual bands. Pertinent numerical values from both the solution and the crystal spectra are listed in Table 1. The numbers for the two weak transitions carry relatively large uncertainty owing to their weak nature.

Oriented Gas Analysis. In order to deduce transition moment directions, the analysis of the absorption spectra will first follow the oriented gas model in which intermolecular interactions along with the concomitant intensity mixing are ignored. Although the mixing of states due to crystal interactions alters dichroic ratios and thus the apparent transition moment directions, it is reasonable to neglect these effects initially. For glutarimide with near C_{2v} symmetry of the imide chromophore we expect transitions to be polarized very close to the *x*, *y*, or *z* molecular axes. These three vector types are projected onto the *a*, *b*, and *c* crystal axes, and component oscillator strengths evaluated. The ratios of the latter values are termed *dichroic ratios* and are used as

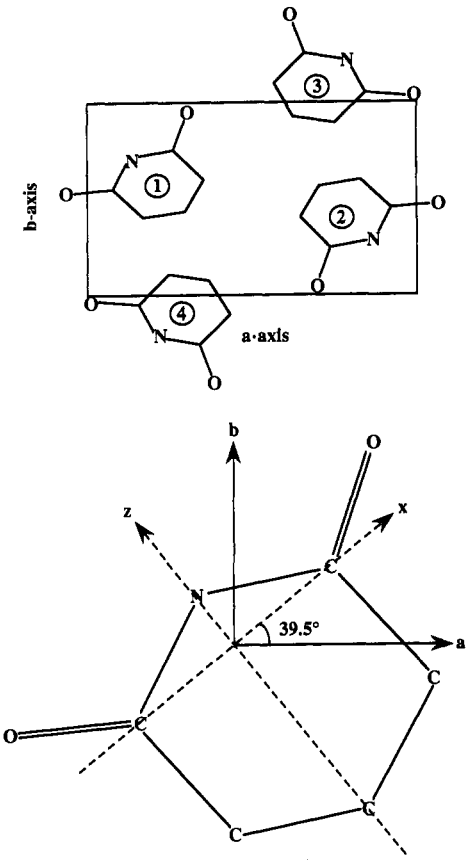

Figure 5. (Top) Projection of the four molecules in the unit cell onto the (001) crystal plane and (bottom) an enlarged view of the site 1 molecule. The molecular coordinate system is defined in Figure 1. All sites in the unit cell are spectroscopically equivalent, and their relative positions are as follows: (site 1) x, y, z; (2) $-x, -y, -z$; (3) $-x, {}^1/_2 + y, {}^1/_2 - z$; (4) $x, {}^1/_2 - y, {}^1/_2 + z$.

benchmarks for assigning polarization directions to observed transitions. Crystal interactions are expected to cause deviations, but such changes are usually not large enough to subvert the basic assignments.

The strong band near 49 000 cm^{-1} (band III) appears most prominently along the *a* and *b* axes. Since the plane of the imide group is close to the *ab* crystal plane (deviation = 8°), we expect that this transition must certainly be in-plane polarized. The projection onto the *ab* face of the four molecules in the unit cell and an enlarged diagram of one molecule (site 1) are shown in Figure 5. The projection of an *x*-axis vector in the molecule forms an angle of 39.5° with the *a* axis. The two possible in-plane, symmetry-defined transition moment directions, *x* or *z*, are therefore expected to show dichroic ratios $f_a{:}f_b$ of 1.47 or 0.66, respectively. The experimental value of 1.32 indicates *x*-axis polarization for this transition. The weaker *c*-axis component also supports this assignment. The oriented gas dichroic ratio $f_b{:}f_c$ is 4.5 for *x* polarization and 29 for *z* polarization; the experimental value is 3.4. Therefore with confidence, we assign this transition as polarized along the *x* molecular axis.

Because of their inherent weakness the bands at 39 000 and 45 000 cm^{-1} are very susceptible to significant changes in dichroic ratio arising from Herzberg–Teller coupling (*vide infra*). Nevertheless, for transition II the observed dichroic ratios ($f_a{:}f_b{:}f_c$) are (0.032:0.026:0.012) or (1.2:1.0:0.46) and are close to the values for *x* polarization (1.47:1.00:0.66). The component intensities for transition I are too weak to claim more than that the intensities are comparable along the three axes. However, when the directly measured absorption edges of the (100) face are examined, it is clear that the *c*-polarized absorption rises more rapidly than that along the *b* axis. The only polarization type that is consistent with this observation is *y*. We therefore tentatively assign *y* and *x* polarization to I and II, respectively.

Table 2. Inner Dipolar Lattice Sums t_{ij} for Unit Vectors Directed along the Various Crystallographic Axes[a] (cm^{-1} $Å^{-2}$)

	site combinations[b]			
	1,1	1,2	1,3	1,4
aa	−136	−1193	−1759	3356
bb	−1267	−935	−1264	2397
cc	−1360	−243	168	−9056
ac	302	−573	514	1947
bc	0	−228	0	0
ab	0	−425	0	0

[a] The dipole position is taken to be the center of mass of the imide group. [b] The other site combinations are related to those given as follows: 1,1 = 2,2 = 3,3 = 4,4; 1,2 = 2,1 = 3,4 = 4,3; 1,3 = 3,1 = 2,4 = 4,2; 1,4 = 4,1 = 2,3 = 3,2.

The absorption in the vicinity of 70 000 cm^{-1} cannot be resolved into individual bands, owing to the general diffuseness. The region is likely to be composed of multiple, overlapping bands. Considering the relative intensities along the *a*, *b*, and *c* axes it seems reasonable to suppose that the bulk of the intensity is derived from in-plane-polarized bands.

Summarizing the above conclusions we assign the three transitions observed in the glutarimide spectrum as follows: I, 40 200 cm^{-1} (249 nm), $f = 0.001$, *y* polarization; II, 44 800 cm^{-1} (223 nm), $f = 0.007$, *x* polarization; and III, 49 800 cm^{-1} (201 nm), $f = 0.30$, *x* polarization. The values for the oscillator strengths and energies are taken from the aqueous solution spectrum, and the polarization assignments relate to axes for the local C_{2v} symmetry of the imide moiety.

Intermolecular Interactions. In spite of the above agreement between experimental dichroic ratios and oriented gas predictions for the dominant *x*-polarized transition, one may still question whether crystal interactions might produce similar results for a *z*-polarized transition and therefore confuse the assignment. Furthermore, the Davydov shift to higher energy and the obvious distortion of the band shape of the *c*-axis component of III suggests that crystal interactions are not negligible. Such results are frequently observed in crystal spectra.[11,13,21,22] In an effort to settle the issue we have calculated the approximate energy and intensity shifts that result from the crystal field interactions by carrying through exciton mixing calculations for various scenarios. These calculations show strong support for the assignment of III as having *x* polarization.

The theory for treating intermolecular interactions in molecular crystals has been described previously.[23] The multipole expansion of the intermolecular interactions in the crystal is truncated to include only transition dipole–transition dipole terms. These terms appear as dipole–dipole lattice sums. Terms in the expansion involving permanent dipole moments in both ground and excited states are ignored since there are no data available regarding their magnitudes. The necessary sums evaluated with the Ewald–Kornfeld procedure[24] for unit dipoles (1 Å) directed along the unit cell axes are listed in Table 2. Any particular dipole lattice sum can be evaluated from the numbers given. Macroscopic (or long-range) terms appropriate for the individual crystal faces considered must be added to obtain the final overall lattice sum.

Crystal calculations based on the model spectrum given at the end of the last section can be carried through in a variety of ways. The simplest approach is to treat a three-state problem in the strong coupling limit. Here the oscillator strength of each transition is concentrated at the center of the absorption bands and separate calculations for the (001) and (100) faces are performed. The results of this approach are given in Table 3.

(21) Clark, L. B. *J. Am. Chem. Soc.* **1986**, *108*, 5109.
(22) Clark, L. B. *J. Phys. Chem.* **1990**, *94*, 2873.
(23) Chen, H. H.; Clark, L. B. *J. Chem. Phys.* **1973**, *58*, 2593.
(24) Kornfeld, H. *Z. Phys.* **1924**, *22*, 27.

Table 3. Comparison of Calculated and Experimental Crystal Spectra[a,b]

	a axis		*b* axis		*c* axis	
	f	ν (cm^{-1})	*f*	ν (cm^{-1})	*f*	ν (cm^{-1})
			Oriented Gas			
I	0.00005	39 000	0.00002	39 000	0.003	39 000
II	0.0004	45 000	0.0001	45 000	0.02	45 000
III	0.52	50 000	0.36	50 000	0.09	50 000
			Interactions			
I	0.00002	39 003	0.0001	39 011	0.003	38 978
II	0.018	44 972	0.011	44 978	0.001	45 038
III	0.51	49 103	0.35	49 288	0.086	52 085
			Experimental			
I	~0.005	38 900	~0.005	39 000	~0.005	41 000
II	0.032	45 100	0.026	44 800	0.012	44 400
III	0.58	49 500	0.44	48 800	0.13	52 200

[a] The input data for the oriented gas results and for the crystal calculations are obtained from the aqueous solution spectrum. [b] Oscillator strengths are one-dimensional values.

Table 4. Transition Energies, Wavelengths, Oscillator Strengths, and Transition Moment Directions from SCI and SDCI of INDO/S

	ν (10^3 cm^{-1})			*f*			polarization[a]		
band	I	II	III	I	II	III	I	II	III
standard SCI	29.7	31.0	50.1	0.0008	0.0001	0.53	*y*	*x*	*x*
SDCI, $f_\pi = 0.55$			49.5			0.57			*x*
SCI, π only			48.7			0.46			*x*
SDCI, $f_\pi = 0.66$			57.2			0.69			*x*

[a] The axes are defined in Figure 1.

Relative to the oriented gas values the calculated changes arising from the crystal field are minimal. The one exception is the strong blue shift (~2000 cm^{-1}) of the *c*-axis component of III. In fact, just such a shift is observed. Calculations made assuming *z* polarization for III again show only slight changes in the dichroic ratio for *z* polarization. We are forced to conclude that crystal interactions cannot modify a formally *z*-polarized transition into one resembling an *x*-polarized transition.

A second calculation can be carried out in the weak coupling limit wherein III is decomposed into a number of individual vibronic components. We find that when III is decomposed into five equally spaced components, the intensity shifts among these components to yield an overall shift of peak intensity that closely resembles the strong coupling result. Other calculations have been made in which higher energy bands were arbitrarily included to represent the absorption intensity near 70 000 cm^{-1}. Again the effects of including of such bands are minimal, and the results are substantially similar to those shown in Table 3. We therefore conclude that crystal interactions cannot overturn the conclusions drawn from the oriented gas analysis given above.

MO Calculations. The molecular coordinates used in the calculations are taken from the crystal structure of Petersen.[12] Although the molecular structure in the crystal shows approximate C_{2v} local symmetry, the calculations reflect the actual C_1 symmetry (no symmetry elements other than the identity) of the crystal environment. Table 4 lists transition energies, wavelengths, oscillator strengths, and transition moment directions predicted by the several SCI and SDCI calculations. In the standard SCI run, the CI includes 196 singly excited configurations generated from the 14 highest occupied MO's and the 14 lowest empty MO's. The energy of the lowest $\pi \rightarrow \pi^*$ transition is close to that of the principal experimental band (III) if the standard interaction factors recommended by Zerner for the SCI calculations are used. However, in the SDCI calculations, it is necessary to modify the values of this parameter in order to force agreement between experiment and theory.

In the SDCI calculations, all 22 occupied MO's and all 17 unoccupied MO's are included. This set generates eight singly and 28 doubly excited $\pi\pi^*$ configurations. When the parameter f_π is set equal to 0.55, the predicted position of the lowest $\pi\pi^*$ band is near to the experimental peak position for transition III. The polarization for this transition is always in the *x* direction. The standard SCI calculation yields two weak transitions below the energy of the dominant $\pi\pi^*$ transition. This result is consistent with the two weak bands observed in the solution spectra, although the energies of the calculated transitions are quite different from the experimental ones.

The standard SCI calculation shows that the major contribution to transition I is ψ_{22} (the 22nd molecular orbital, HOMO) $\rightarrow \psi_{23}$ (LUMO, CI coefficient 0.843); transition II is $\psi_{20} \rightarrow \psi_{23}$(CI coefficient 0.631) and $\psi_{22} \rightarrow \psi_{24}$ (CI coefficient 0.641); transition III is $\psi_{21} \rightarrow \psi_{23}$ (CI coefficient 0.825). The major atomic orbital components of the MO's obtained from the SCI calculations are

$$\psi_{25} = 0.42s(C_5) - 0.37s(C_4) + 0.36s(C_1) - 0.34s(N_8) - 0.29s(C_2) + 0.25s(C_3) + \ldots$$

$$\psi_{24} = 0.56p_y(C_1) + 0.56p_y(C_5) - 0.37p_y(N_8) - 0.32p_y(O_6) - 0.32p_y(O_7) + \ldots$$

$$\psi_{23} = 0.59p_y(C_1) - 0.58p_y(C_5) - 0.38p_y(O_6) + 0.38p_y(O_7) + \ldots$$

$$\psi_{22} = -0.56p_z(O_6) + 0.51p_z(O_7) - 0.40p_x(O_6) - 0.36p_x(O_7) + \ldots$$

$$\psi_{21} = -0.58p_y(N_8) + 0.45p_y(O_6) + 0.43p_y(O_7) + \ldots$$

$$\psi_{20} = -0.49p_z(O_7) - 0.46p_z(O_6) + 0.26p_x(O_7) - 0.23p_x(O_6) + \ldots$$

$$\psi_{19} = 0.59p_y(O_7) - 0.56p_y(O_6) + 0.33p_y(C_1) - 0.33p_y(C_5) + \ldots$$

$$\psi_{18} = 0.44p_y(C_3) + 0.36p_y(N_8) - 0.35p_y(C_4) - 0.33p_y(C_2) + \ldots$$

ψ_{20} (which also carries some character of ψ_{21}) and ψ_{22} are essentially the in-phase and out-of-phase combinations respectively of the nonbonding orbitals occupied by the lone pairs in two oxygem atoms. ψ_{18}, ψ_{19}, and ψ_{21} are π orbitals; ψ_{23} and ψ_{24} are π^* orbitals; ψ_{25} is σ^* orbital. The symmetry species of these orbitals can be deduced from the above LCAO's, and they are b_2, a_2, a_1, b_2, b_1, a_2, b_2, and a_1, respectively in the approximate C_{2v} symmetry. The predicted polarization appropriate for the local C_{2v} symmetry of the imide group are given in Table 4.

Discussion

The sequence of the π-type orbitals obtained from the SCI calculations is in accord with basic expectations. The orbital energy level diagram is given in Figure 6 where the symmetry labels shown apply to the local C_{2v} symmetry. Transition I arises principally from the excitation of an electron from ψ_{22} (out-of-phase combination of the oxygen 2p nonbonding orbitals) to ψ_{23} (out-of-phase combination of the localized π^* MO of the carbonyl groups). Although it is formally allowed with *y* polarization, it is expected to be very weak with an intensity similar to the $n\pi^*$ band of amides.[25] Upon lowering the symmetry to C_S (correct for glutarimide), this band can mix with other possible *z*-polarized transitions to some extent, and this expectation is shown by the

(25) Robin, M. B. *Higher Excited States of Polyatomic Molecules*; Academic: New York, 1975; Vol. II.

Table 5. Effect of Geometry on Calculated Transition Moment Vectors (D)[a]

	C_{2v}	C_s				C_1			
transition		f	x	y	z	f	x	y	z
I	y	0.0008	0.000	0.241	−0.024	0.0008	0.008	0.238	−0.026
II	forbidden	2×10^{-6}	0.012	0.000	0.000	5×10^{-5}	−0.055	0.020	0.001
III	x	0.53	4.76	0.000	0.000	0.53	4.75	0.059	0.042

[a] Oscillator strengths are three-dimensional values.

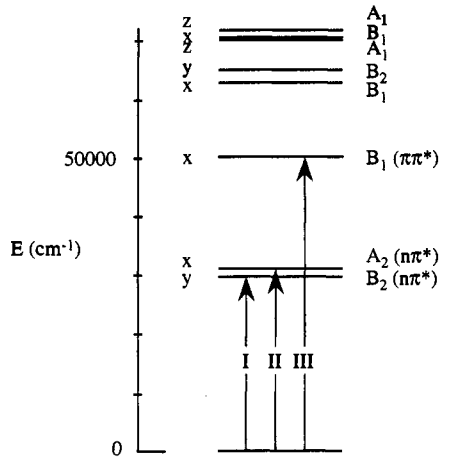

Figure 6. Energy level diagram for glutarimide obtained from MO calculations. The symmetry labels shown are for the approximate C_{2v} symmetry of the imide group. Polarization directions shown refer to the actual C_S symmetry of the glutarimide molecule.

semiempirical MO calculations for a geometry adjusted to reflect C_S symmetry. The effect on the transition moment direction due to the out-of-plane methylene group is rotation by 6° away from the central methylene group. Calculations based on the further slight distortion of the structure to the actual crystal coordinates of glutarimide show a further small shift of less than 2°. The coordinates of these vectors are given in Table 5 for mutual comparison. Transition I is in all cases predicted to be very weak ($f = 0.0008$).

The second predicted transition is an $n\pi^*$ band involving extensive configuration interaction. There are almost equal contributions from $\psi_{22} \rightarrow \psi_{24}$ ($n_2 \rightarrow \pi_5^*$) and $\psi_{20} \rightarrow \psi_{23}$ ($n_1 \rightarrow \pi_4^*$) together with a hefty component of $\psi_{21} \rightarrow \psi_{23}$ ($\pi_3 \rightarrow \pi_4^*$) and lesser components of many other configurations. Although such a transition is formally forbidden in C_{2v} symmetry, it is weakly allowed in the actual C_S symmetry of the glutarimide molecule ($f = 2 \times 10^{-6}$, x polarization). Upon reducing the symmetry to that in the crystal the calculated intensity gains slightly ($f = 5 \times 10^{-5}$), and the direction changes about 20° from pure x toward the y axis.

While such theoretical calculations of the effects of slight changes in geometry on the oscillator strengths and transition moment directions are interesting and useful in gauging the magnitudes of such effects, it must be remembered that the observed intensities for very weak bands may be unrelated to any such analysis. Herzberg–Teller mixing from other allowed transitions no doubt confuse the issue owing to the borrowing of so-called *forbidden intensity* in nominally allowed, weak transitions.[26,27] If the allowed component of a transition is inherently small, then the borrowed intensity may even dominate. The original state symmetry is then obscured, and observed dichroic ratios reflect the borrowed intensity and not the symmetry of the state in question. It is therefore to be expected that weak bands may exhibit mixed polarization. Transition I is too weak to obtain accurate dichroic ratios. The absorption edge data for the (100) face can be reasonably interpreted as a y-polarized band containing a substantial x-polarized component. Transition II is formally allowed with x polarization. Since there is no nearby, strong transition with another polarization, it is expected that II will not show significant mixed polarization. Within experimental uncertainty it does not.

The results of calculations for band III are hardly affected by the geometry changes indicated above. This transition is polarized perpendicular to the mirror plane in both C_{2v} and C_S symmetry. Upon reducing the symmetry to that in the crystal environment the vector direction of III changes by less than 1°. These results are indicated in Table 5.

Other calculated higher energy states are shown in Figure 6. Only excited configurations reached from the ground state with oscillator strengths greater than 0.01 are shown, for there is considerable congestion in this region. When these predicted transition moment vectors are projected onto the crystal axes and the component oscillator strengths summed, then the calculated relative intensities are near those observed.

The MO results for the energies of the two $n\pi^*$ bands are uniformly low by about 10 000 cm^{-1}. Since it is known that hydrogen-bonding environments usually cause modest blue shifts of such transitions, and since both the aqueous solution and the crystal environment involves hydrogen bonding of the carbonyl lone pairs, could it be that the discrepancy between theory and experiment with regard to the energies of these transitions is explained in this simple way? To investigate this question the absorption spectrum of glutarimide dissolved in trimethyl phosphate (which contains no hydrogen atoms available for hydrogen bonding) was measured. No appreciable shifts of these bands occur. Again, the spectrum of glutarimide dissolved in heptane (unknown concentration) showed the same two unshifted bands. Finally, MO calculations were carried through that included water molecules strategically placed near the oxygen atoms of glutarimide.[28] Little if any movement of the positions of the $n\pi^*$ bands were obtained. We conclude that the parametrization of the semiempirical calculations is adequate for computing the $\pi\pi^*$ transitions but fails to accurately yield the energies of $n\pi^*$ bands for glutarimide.

Acknowledgment. We thank Professors Patrik Callis and Michael Zerner for providing the ZINDO program and some other utility programs. We also thank Dr. P. Gantzel for the determination of crystal faces using X-ray diffraction technique. This work was supported by National Institutes of Health grant no. GM38575.

(26) Herzberg, G.; Teller, E. *Z. Phys. Chem.* **1933**, *21*, 410.

(27) Michl, J.; Thulstrup, E. W. *Spectroscopy with Polarized Light*; VCH Publishers: New York, 1986.

(28) Huheey, J. E. *Inorganic Chemistry*, 3rd ed.; Harper & Row: New York, 1983; p 268.